Ganoderic acid T inhibits tumor invasion *in vitro* and *in vivo* through inhibition of MMP expression

Nian-Hong Chen[1,2], Jian-Wen Liu[2,3], Jian-Jiang Zhong[1,2]

[1]Key Laboratory of Microbial Metabolism, Ministry of Education, School of Life Sciences and Biotechnology, Shanghai Jiao Tong University, 800 Dong-Chuan Road, Minhang, Shanghai 200240, China

[2]State Key Laboratory of Bioreactor Engineering, East China University of Science and Technology, 130 Meilong Road, Shanghai 200237, China

[3]School of Pharmacy, East China University of Science and Technology, 130 Meilong Road, Shanghai 200237, China

Correspondence: Jian-Jiang Zhong, e-mail: jjzhong@sjtu.edu.cn; Nian-Hong Chen, e-mail: nhchen1224@yahoo.com.cn

Abstract:

The traditional Chinese medicinal mushroom, *Ganoderma lucidum*, has been used in Asia for several thousand years for the prevention and treatment of a variety of diseases, including cancer. In previous work, we purified ganoderic acid T (GA-T) from *G. lucidum* [28]. In the present study, we investigate the functions of GA-T in terms of its effects on invasion *in vitro* and metastasis *in vivo*. A trypan blue dye exclusion assay indicates that GA-T inhibits proliferation of HCT-116 cells, a human colon carcinoma cell line. Cell aggregation and adhesion assays show that GA-T promotes homotypic aggregation and simultaneously inhibits the adhesion of HCT-116 cells to the extracellular matrix (ECM) in a dose-dependent manner. Wound healing assays indicate that GA-T also inhibits the migration of HCT-116 cells in a dose-dependent manner, and it suppresses the migration of 95-D cells, a highly metastatic human lung tumor cell line, in a dose- and time-dependent manner. In addition, GA-T inhibits the nuclear translocation of nuclear factor-κB (NF-κB) and the degradation of inhibitor of κB-α (IκBα), which leads to down-regulated expression of matrix metalloproteinase-9 (MMP-9), inducible nitric oxide synthase (iNOS), and urokinase-type plasminogen activator (uPA). Animal and Lewis Lung Carcinoma (LLC) model experiments demonstrate that GA-T suppresses tumor growth and LLC metastasis and down-regulates MMP-2 and MMP-9 mRNA expression *in vivo*. Taken together, these results demonstrate that GA-T effectively inhibits cancer cell invasion *in vitro* and metastasis *in vivo*, and thus it may act as a potential drug for treating cancer.

Key words:
ganoderic acid T, metastasis, invasion, MMP-9, uPA

Abbreviations: ANOVA – analysis of variance, ECM – extracellular matrix, MMP – matrix metalloproteinase, RT-PCR – reverse transcription polymerase chain reaction, SDS-PAGE – sodium dodecyl sulfate polyacrylamide gel electrophoresis

Introduction

Ganoderma lucidum (Fr.) Karst (Polyporaceae), a traditional Chinese medicinal mushroom, has been used for centuries in East Asia to prevent and treat a variety of diseases, such as immunological disorders and cancers [2, 24, 28]. A mixture of extracts and/or purified compounds from *G. lucidum* have been documented to suppress proliferation; induce cell cycle arrest and apoptosis; and inhibit angiogenesis, invasion or metastasis of human and mouse carcinoma cell lines and in mice [6, 7, 12, 13, 17, 20, 25, 26, 30, 33, 34]. The compound(s) responsible for the bioactivities in these extract mixtures is unclear, making the study of structure-activity relationships difficult. Therefore, the use

of a purified triterpene is required to reveal the mechanism of the responsible compounds and to further screen and rationally design structurally similar compounds. Until now, over a hundred ganoderma triterpenes have been identified from *G. lucidum*. Of these ganoderma triterpenes, lucidenic acid B has been shown to inhibit cell growth and apoptosis in HL-60 cells [9]. Ganoderic acid (GA) X induced apoptosis in HuH-7 cells, a human hepatocellular carcinoma, and inhibited the activity of topoisomerases [14]. GA-D possessed a cytotoxic effect on HeLa cells, a human cervical cancer cell line [35]. GA-Me inhibited tumor growth and lung metastasis of LLC cells by enhancing the immune function *in vivo* [32], inhibited tumor invasion by down-regulating gene expression of matrix metalloproteinases (MMP)-2 and MMP-9 [2]. GA-T inhibited tumor growth of 95-D cells [28]. GA-A and GA-H suppressed cell adhesion, migration and invasion, as well as inhibited secretion of urokinase-type plasminogen activator (uPA) in MDA-MB-231 cells by inhibiting the transcription factors, activator protein 1 (AP-1) and nuclear factor-κB (NF-κB) [11].

MMPs, including the gelatinases MMP-2 and MMP-9, are a family of secreted or transmembrane proteins that can degrade the proteins of the extracellular matrix (ECM). MMPs have been implicated in many abnormal physiological conditions, including cancer invasion, metastasis and angiogenesis [1]. uPA is a serine protease that converts inactive plasminogen to active plasmin. uPA cleaves several components of the ECM and is also involved in cell adhesion and migration [11, 25]. In addition, uPA is involved in tumor angiogenesis by directly, or *via* plasmin formation, leading to the release or activation of many angiogenic growth factors such as basic fibroblast growth factor (bFGF) and vascular endothelial growth factor (VEGF) [19]. Taken together, MMP-2/9 or uPA apparently play an important role in tumor invasion and metastasis [11, 15]. Nitric oxide (NO), an endothelial growth factor, specifically mediates tumor vascularization to regulate blood flow. The production of NO from inducible nitric oxide synthase (iNOS) is associated with the suppression of tumor development and inhibition of cancer cell metastasis *in vitro* and *in vivo* [10].

NF-κB is a transcription factor that exists as a homodimer or a heterodimer of five subunit proteins including RelA (p65), NF-κB1 (p50/p105), NF-κB2 (p52/p100), c-Rel, and RelB. The p65:p50 heterodimer is the dominant form of NF-κB, which regulates the expression of related invasion/metastasis genes (such as MMP-2/9, uPA, and iNOS) [4, 10, 11, 15, 19] and genes involved in angiogenesis (such as iNOS) [27]. NF-κB is inactive when bound by the inhibitory protein, inhibitor of κB (IκB), in the cytoplasm. Once cells are stimulated by extracellular factors, such as growth factors, carcinogens, and/or oxidative stress, IκB is subsequently phosphorylated by IκB kinase, ubiquitinated by an E3 ligase, and degraded by the proteasome to release NF-κB [11, 15, 18, 21, 27]. Released NF-κB moves into the nucleus and binds to the promoter region of target genes to activate gene expression [18, 21, 22, 27]. The activation of NF-κB target genes influences cell proliferation and cell survival pathways which promote tumorigenesis and increase the chemoresistance of cancer cells. Therefore, inhibition of NF-κB activation, which down-regulates MMP-2/9, uPA and iNOS genes, may reduce the risk of cancer development and support chemotherapeutics by inhibiting invasion and metastasis.

However, the precise molecular mechanisms by which GA-Me inhibits tumor cell invasion *in vitro* and metastasis *in vivo* remains unknown. GA-Me inhibited tumor invasion by down-regulating MMP-2/9 gene expression *in vitro* and inhibited tumor growth and lung metastasis of Lewis Lung Carcinoma (LLC) cells [2, 32]. In addition, although GA-A and GA-H suppressed MDA-MB-231 invasion by inhibiting of AP-1 and NF-κB, the anti-invasion efficacy of GA-A and GA-H was limited (at 0.25 mM for 24 h, GA-A and GA-H reduced the invasion of MDA-MB-231 cells to 49.9% and 50% of the control, respectively). Moreover, it is unclear whether GA-A and GA-H possess an anti-metastatic function *in vivo* and the molecular mechanism of this anti-metastatic function of GA-A and GA-H *in vivo* remains unknown [11]. Until now, it was unclear whether GA-T possesses an anti-invasion and anti-metastasis function and the molecular mechanism by which GA-T may mediate these functions remains unknown. Therefore, in the present study, we wanted to investigate the molecular mechanism of the anti-invasion/anti-metastasis function of GA-T *in vitro* and *in vivo*.

Materials and Methods

All animal procedures conform to the Guide for the Care and Use of Laboratory Animals published by the

United States National Institutes of Health (NIH Publication No. 85–23, revised 1996), and the Guidelines for Animal Care and Treatment of the People's Republic of China. Experimental procedures used in the present study were approved by the local East China University of Science and Technology and Shanghai Jiao Tong University Ethical Committee on Animal Experiments.

Materials

RPMI 1640, Trizol reagent and 3-(4,5-dimethylthiazol-2-yl)-2,5-diphenyltetrazolium bromide (MTT) were obtained from GIBCO Industries, Inc. (Invitrogen, Carlsbad, CA, USA.). Matrigel® was obtained from Becton Dickinson Labware (Bedford, MA, USA). McCoy's 5A Modified Medium, Dimethyl sulfoxide (DMSO) and glutaraldehyde were obtained from Sigma (St. Louis, MO, USA). New bovine serum (NBS) and antibiotics (penicillin and streptomycin) were purchased from Sino-American Biotechnology Co. (Shanghai, China). Tumor necrosis factor-α (TNFα) was purchased from ProSpec-Tany TechnoGene Ltd. (Rehovot, Israel). Antibodies for actin, MMP-9, uPA, p65, IκBα, and *iNOS* were purchased from Santa Cruz Biotechnology (Santa Cruz, CA, USA). Poly-vinylidene fluoride (PVDF) membrane, phenylmethylsulfonyl fluoride, sodium orthovanadate, leupeptin, aprotinin, β-mercaptoethanol, 4-(2-hydroxyethyl)-1-piperazineeth-anesulfonic acid (HEPES), and dithiothreitol (DTT) were purchased from Amresco (Solon, Ohio, USA). Goat anti-rabbit IgG-conjugated to horseradish peroxidase (HRP) and rabbit anti-goat IgG-conjugated to HRP were purchased from Biovision (Mountain View, CA, USA), BM Chemiluminescence Blotting Substrate (POD) substrate reagents were purchased from Roche Diagnostics (Yerevan, USA). The Reverse Transcription System was purchased from Promega Corporation (Madison, WI, USA). The 2×SYBR pre-mix Ex Tap^{TM} perfect real-time PCR version and RNase-free DNase I were obtained from TaKaRa Biotechnology Co., Ltd. (Dalian, China). Cisplatin was purchased from Shanghai Hua Lian MediPharma Ltd. (Shanghai, China).

GA-T was purified with semi-preparative liquid chromatography in our lab to a purity over 99% [28]. The structure of the compound is shown in Figure 1. Stock solutions of GA-T were prepared in DMSO and stored at –20°C. Further dilutions were made with RPMI 1640 medium or McCoy's 5A Modified Me-dium immediately before use. The final concentration of DMSO was less than 0.1%.

Cell culture

The highly metastatic human lung tumor cell line 95-D was from the Cell Bank of the Chinese Academy of Science. 95-D cells were cultured in RPMI Medium 1640, while the human colon carcinoma cell line HCT-116 was cultured in McCoy's 5A Modified Medium, plus 10% (v/v) dialyzed heat-inactivated NBS, 100 units/ml penicillin, and 100 units/ml streptomycin at 37°C in a humidified atmosphere of 95% air and 5% CO_2.

Cell survival assay

HCT-116 cells were plated at a concentration of 10^6 cells/ml in 6-well Costar plates in McCoy's 5A Modified Medium at 37°C for 4 h in a 95% O_2, 5% CO_2 incubator. Triplicate wells of the cells were then treated with either 0 µM (0.5 µl/ml of DMSO in the medium), 8.2 µM (5 µg/ml), 12.3 µM (7.5 µg/ml), or 16.3 µM (10 µg/ml) of GA-T for 24 h. The cells were stained with trypan blue (Invitrogen, Carlsbad, CA, USA) and counted under the microscope after the cells were harvested by trypsinization (Amresco, Solon, Ohio, USA) [1, 22]. Significant differences between the groups was evaluated using one-way analysis of variance (ANOVA) followed by Dunnett's multiple comparison test.

Wound healing assay

Wounding healing assays were performed as previously described [2, 36]. Briefly, HCT-116 or 95-D cells were plated in 24-well microtiter cell culture plates for 24 h in 0.5 ml of McCoy's 5A Modified Medium (or RPMI 1640 Medium for the 95-D cells) containing 10% (v/v) NBS. After the cells formed a confluent monolayer, the cells were scraped with a pipette tip and the cells were cultured in McCoy's 5A Modified Medium containing either different concentrations of GA-T or doxycycline (Dox, as the positive control). After 24 h, the cell migration distance was examined. Measurements of the wound width were made at the beginning of the experiment and after 24 h. Measurements were made at 40× magnification using an ocular grid. Significant differences between the groups was evaluated using one- or two-

way ANOVA followed by Dunnett's multiple comparison test.

Cell adhesion assay

Cell adhesion assays were performed essentially as previously described [2, 36]. Briefly, the HCT-116 cell lines were pre-treated with or without different concentrations of GA-T or Dox (as the positive control) for 18 h. The HCT-116 cell lines were suspended in serum-free McCoy's 5A Modified Medium to form a single-cell suspension and 2×10^6 cells/ml (2×10^5 cells/well) were seeded into 96-well microtiter cell culture plates pre-coated with Matrigel®. After a 45 min incubation at 37°C, the wells were washed three times with PBS to remove non-adherent cells and 10 µM MTT was added into each well for an additional 4 h. The blue MTT formazan precipitate was dissolved in 100 µl of DMSO. As a measure of cell viability, the absorbance at 570/630 nm was taken using a microplate reader model Multiskan Mk3. Significant differences between the groups was evaluated using one-way ANOVA followed by Dunnett's multiple comparison test.

Cell aggregation assay

Cell aggregation assays were performed essentially as previously described [2, 36]. Briefly, a single-cell suspension was obtained using a standard trypsinization procedures. A total of 2×10^5 cells in 1 ml of McCoy's 5A Modified Medium (serum-free) with or without different concentrations of GA-T or Dox (as the positive control) were placed in polystyrene microtubes and were gently shaken every 5 min for 1 h at 37°C. At the end, glutaraldehyde (at a final concentration of 2% (v/v)) was added to stop the aggregation process. Homotypic aggregation was evaluated microscopically in a hemocytometer by counting only single, non-aggregating cells. Percent of aggregated cells was calculated as: $(1 - Ne/Nc) \times 100\%$, where Ne is the number of single cells with or without different concentrations of GA-T or Dox after incubation at 37°C and Nc is the number of single cells before incubation (after the standard trypsinization procedure). Significant differences between the groups were evaluated using one-way ANOVA followed by Dunnett's multiple comparison test.

Preparation of cell extracts and western blot analysis

HCT-116 cells (1×10^6) were placed in a culture dish (10 cm) and treated with 32.6 µM of GA-T for 0, 12 or 24 h. HCT-116 cells were also treated with or without (only DMSO) different concentrations of GA-T for 24 h. Total populations of cells, including adherent and floating cells were washed with PBS twice and resuspended at 10^6 cells/10 ml in hypotonic solution [10 mM HEPES (pH 7.9), 10 mM KCl, 2 mM $MgCl_2$, 1 mM DTT, 0.1 mM EDTA, 0.1 mM phenylmethylsulfonyl fluoride (PMSF), 1 mM sodium orthovanadate, 10 mM NaF, 5 mM leupeptin, and 10 µg/ml aprotinin]. The cytoplasmic and nuclear fraction extracts were obtained using a procedure previously described [3, 8]. Total protein extracts were obtained using a procedure previously described [2, 28]. All samples were stored at –80°C until use.

Equal amounts of proteins (40–60 µg) were separated by 10% SDS-polyacrylamide gels electrophoresis and transferred to a PVDF membrane (Amresco, USA). After blocked, the PVDF membrane was sequentially probed with an anti-MMP-9 (diluted 1:750), anti-p65 (diluted 1:1000), anti-IκBα (diluted 1:1250), uPA (diluted 1:500) and the appropriate secondary antibody conjugated to HRP (diluted 1:5000). The blots were visualized with BM Chemiluminescence Blotting Substrate (POD) reagents. Total cellular protein was determined using the Bradford method [2, 8, 28].

Anti-tumor and anti-metastasis studies of LLC *in vivo*

Eight-week-old male C57B/6 mice were purchased from SLAC Laboratory Animal Co. Ltd. (Shanghai, China). All animal experiments were performed as detailed previously [28, 32]. The animals were implanted with 1×10^8 cells/ml of LLC cells in 0.1 ml at two flanks per mouse. The solid tumors were collected after being allowed to develop for three weeks, cut as cubes of $1 \times 1 \times 1$ mm, and then implanted into other mice at two flanks per mouse. The tumor-bearing C57B/6 mice were divided randomly into four groups and each group included seven mice. When the size of the solid tumor in the tumor-bearing mice reached 100 mm^3, the tumor-bearing mice were treated with GA-T *via* celiac injection at the dosage of either 7 mg/kg or 28 mg/kg for 10 days, and then observed for another eight consecutive days. The negative control group was treated with vehicle mixture
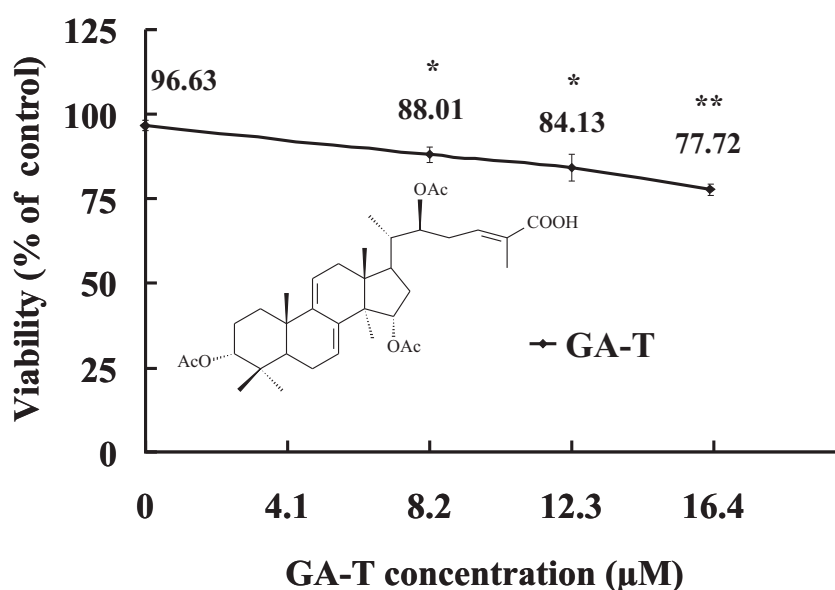
Fig. 1. GA-T inhibits proliferation of HCT-116 cells. HCT-116 cells were incubated with control (DMSO) or with 8.2, 12.3 and 16.3 µM GA-T and the effects on growth were determined using a trypan blue dye exclusion assay as described in the "Materials and Methods". The experiments were repeated three times, all with similar results. The data are presented as the mean ± SD (for each group, n = 4). Statistical significance between untreated and treated cells was determined using one-way ANOVA followed by Dunnett's multiple comparison test where * indicates $p < 0.05$ and ** indicates $p \ 0.01$ *vs.* 0 µM GA-T

only. In the positive surgical group, cisplatin administration (1 mg/kg) was initiated on the first day. The data were statistically analyzed based on solid tumor weight. The rate of inhibition (IR) was calculated according to the formula: IR = [(mean tumor weight of the experimental group – mean tumor weight of the control group) /mean tumor weight of the control group] ×100%.

Lung tissues were also removed and tumor nodes in the surface of lungs were counted under the microscope. The lung metastasis was calculated using the following formula: lung metastatic inhibition rate = [(mean lung metastatic number of the control group - mean lung metastatic number of the treatment group)/mean lung metastatic number of the control group] ×100%.

RNA isolation and real-time PCR

For RNA isolation, 100 mg of the solid tumor tissue from the C57B/6 mice was stored in liquid nitrogen and total RNA was isolated using 1 ml of Trizol reagent following the manufacturer's protocol. First-strand cDNA synthesis and real-time PCR using SYBR Green I dye were performed as previously described [2, 16]. Real-time PCR was performed using 20 µl of a solution containing 2×SYBR *premix Ex Tap*[TM] perfect real-time PCR version and 10 µM of the following specific primers (sense and antisense):

GAPDH,
Sense primer: 5'-AAATGGTGAAGGTCGGTGTG-3'
Antisense primer: 5'-TGAAGGGGTCGTTGATGG-3'

MMP-9,
Sense primer: 5'-GCCCTGGAACTCACACGACA-3'
Antisense primer:
5'- TTGGAAACTCACACGCCAGAAG-3'
MMP-2,
Sense primer:
5'-GATAACCTGGATGCCGTCGTG-3'
Antisense primer:
5'-CTTCACGCTCTTGAGACTTTGGTTC-3'

PCR was carried out in a thermal cycler Rotor-Gene 3000 (Corbett Robotics Inc., San Francisco, CA, USA). Each real-time PCR was performed in triplicate and the level of mRNA expression was calculated and normalized to the level of GAPDH mRNA according to the $2^{-\Delta\Delta Ct}$ method as described by Liva and Schmittgen [2, 16] at each different treatment concentration.

Statistical analysis

Statistical analysis was performed using Student's *t*-test to evaluate the significance of differences between two groups and one-way or two-way ANOVA between three and more than three groups. In all of the graphs, * or # indicates $p < 0.05$, ** or ## indicates $p < 0.01$, and *** or ### indicates $p < 0.001$ between the untreated and the treated cells. All data are expressed as the mean ± standard deviation (SD, for each group n $\ $ 3). One- or two-way ANOVA followed by Dunnett's multiple comparison test was also used for statistical analysis using OriginPro 8 software (Origin Lab Inc.).

Results

Effect of GA-T on adhesion, aggregation and migration of tumor cells

To evaluate the anti-invasion activity of GA-T, we first determined whether the cells could survive GA-T treatment using a trypan blue dye exclusion assay. Cell viability of HCT-116 cells at 0 (DMSO alone), 8.2, 12.3, and 16.3 μM of GA-T for 24 h was 96.63 ± 1.65%, 88.01 ± 1.65%, 84.13 ± 2.18%, and 77.72 ± 1.70%, respectively (Fig. 1). The IC$_{50}$ of GA-T in HCT-116

cells for 24 h is 15.7 ± 2.8 μM (9.6 ± 1.7 μg/mL) by the MTT assay. These data indicate that GA-T inhibits proliferation of HCT-116 cells in a dose-dependent manner.

Cell-cell interactions and cancer cell adhesion to ECM components play important roles in cancer cell invasion and metastasis, as demonstrated in previous studies [2, 11, 19, 36]. To assess the inhibitory effects of GA-T on the adhesion and aggregation of cancer cells, we examined the effects of GA-T on the ability of cancer cells to adhere to ECM proteins (Fig. 2). When the HCT-116 cells were treated with 12.3 μM and 16.3 μM GA-T for 18 h, the adhesion ratios com-

Fig. 2. GA-T affects cancer cell adhesion. HCT-116 cells were treated with different concentrations of GA-T or Dox for 18 h and placed into wells pre-coated with Matrigel®. After a 45 min incubation at 37 C, the percentage of adhering cells was determined by the MTT method. The following equation was used to define the adhesion rate: adhesion rate = (absorbance of the drug treated samples/absorbance of the untreated samples) 100%. The experiments were repeated three times, each with similar results. The data are presented as the mean ± SD (for each group, n = 4). Statistical significance between untreated and treated cells was determine using one-way ANOVA followed by Dunnett's multiple comparison test where * indicates p < 0.05 and ** indicates p < 0.01 *vs.* 0 μM GA-T or # indicates p < 0.05 and ## indicates p < 0.01 vs. 0 μM Dox
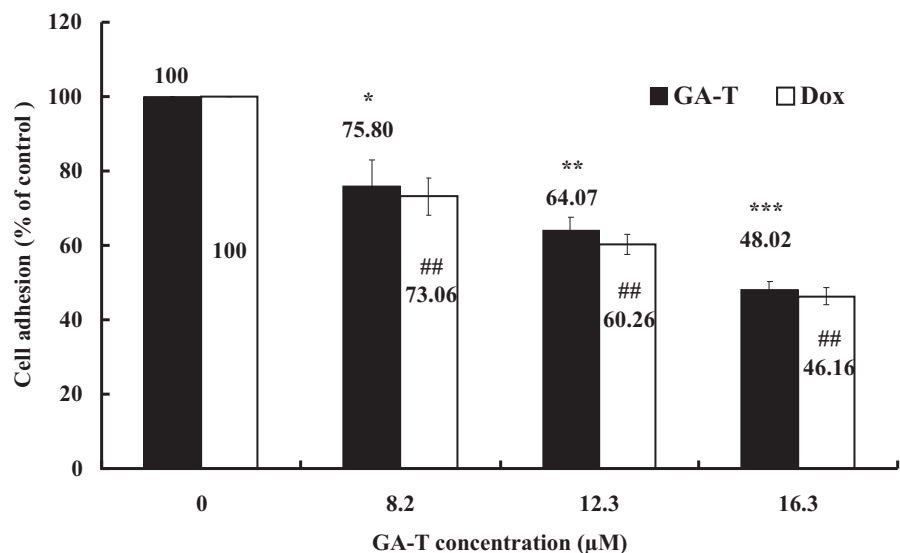

Fig. 3. GA-T enhances cell aggregation. HCT-116 cell suspensions were treated with serum-free McCoy's 5A Modified Medium containing different concentrations of GA-T or Dox for 1 h and the cells were counted. The percent of aggregated cells was determined as described in the "Materials and Methods". Values are the mean ± SD (for each group, n = 4) and the experiment was repeated three times, each with similar results. Statistical significance between untreated and treated cells was determined by one-way ANOVA followed by Dunnett's multiple comparison test where * indicates p < 0.05 and ** indicates p < 0.01 *vs.* 0 μM GA-T or # indicates p < 0.05 and ## indicates p < 0.01 *vs.* 0 μM Dox
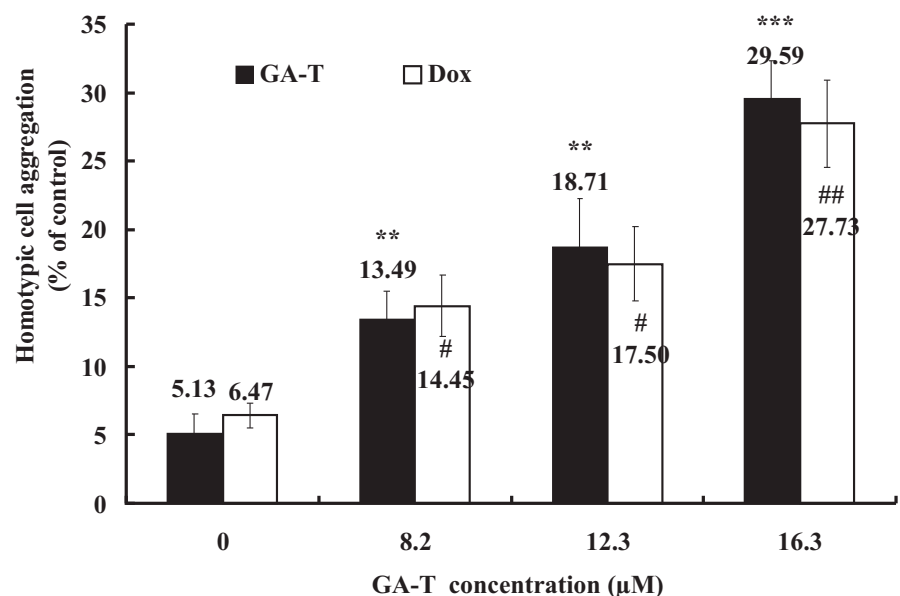
pared to control cells were $64.07 \pm 3.25\%$ ($p < 0.01$) and $48.02 \pm 2.04\%$ ($p < 0.01$), respectively (Fig. 2). Dox (the positive control) also inhibited the adhesion of HCT-116 cells to Matrigel as shown by an inhibition ratio of about $46.16 \pm 2.30\%$ at 16.3 μM. These data indicate that GA-T inhibits Matrigel®-mediated attachment of HCT-116 cells.

Figure 3 shows that GA-T promoted spontaneous HCT-116 cell-cell aggregation in a dose-dependent manner. The percentage of aggregated cells was $29.55 \pm 2.73\%$ ($p < 0.001$) when the cells were treated with 16.3 μM of GA-T for 1 h, which was similar to the Dox (the positive control) stimulated aggregation ratio of $27.72 \pm 3.20\%$ at 16.3 μM. These data indicate that GA-T promotes spontaneous HCT-116 cell-cell aggregation .

Cell migration plays an important role in tumor invasion and metastasis [2, 11, 25, 26, 30, 36]. There-
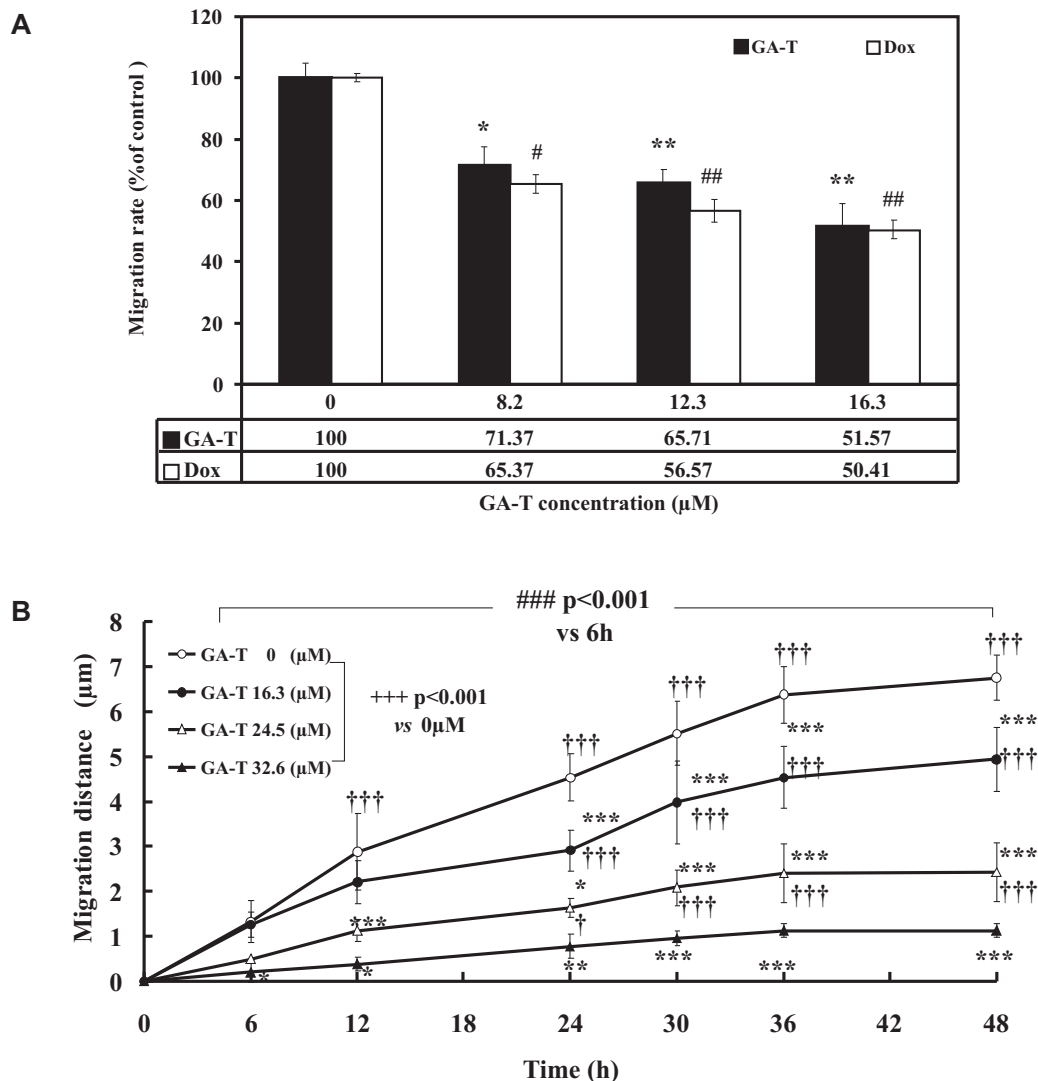

	0	8.2	12.3	16.3
■ GA-T	100	71.37	65.71	51.57
□ Dox	100	65.37	56.57	50.41

Fig. 4. GA-T inhibits cell migration. (**A**) Confluent monolayers of HCT-116 cells were cultured in McCoy's 5A Modified Medium and 0.01% bovine serum albumin (BSA) in the absence and the presence of different concentrations of GA-T or Dox for 24 h after "wounding" of the cell layer with a pipette tip. The data are presented as the mean ± SD (for each group, n = 4). where * indicates p < 0.05 and ** indicates p < 0.01 vs. 0 μM GA-T or # indicates p < 0.05 and ## indicates p < 0.01 vs. 0 μM Dox. (**B**) Confluent monolayers of 95-D cells were cultured in RPMI Medium 1640 and 0.01% BSA in the absence and the presence of different concentrations of GA-T for indicated length of time after "wounding" (for each group, n = 4). Data are expressed as the mean ± SD. Migration distance was statistically analyzed using two-way repeated measures ANOVA (with Dunnett's multiple comparison test) where +++ indicates p < 0.001 vs. 0 μM GA-T and ### indicates p < 0.001 vs. 6 h. The relationship between GA-T concentration and time: * indicates p < 0.05, ** indicates p < 0.01, and *** indicates p < 0.001 vs. 0 μM GA-T at each time and † indicates p < 0.05, †† indicates p < 0.01, and ††† indicates p < 0.001 vs. 6 h at each concentration. One-way and two-way repeated measures ANOVA analyses were performed to determine the significance

fore, we investigated the effect of GA-T on the migration of HCT-116 and 95-D cells. As shown in Figure 4A, GA-T suppresses the migratory capability of HCT-116 cells. Cellular motility of HCT-116 cells was inhibited in a dose-dependent manner by GA-T. Cell migration was suppressed when the HCT-116 cells were treated with 8.2, 12.3, and 16.3 μM GA-T for 24 h. At 16.3 μM, GA-T effectively inhibited the motility of HCT-116 cells ($51.57 \pm 7.37\%$, $p < 0.01$). In comparison, the inhibition ratio of Dox (the positive control) treated HCT-116 cells was about $50.41 \pm 2.93\%$ at 16.3 μM for 24 h. Furthermore, a clear dose-response effect of GA-T was observed.

Compared to untreated controls, GA-T also suppressed the migration capability of 95-D cells (Fig. 4B). Cell migration was suppressed when 95-D cells were treated with 16.3, 24.5, and 32.6 μM GA-T for 24 h. A clear dose–response effect of GA-T was observed. Additionally, GA-T (16.3 μM, as an example) inhibited cell motility effectively at 6 h intervals. In summary, cellular motility of 95-D cells was obviously inhibited in a dose- and time-dependent manner by GA-T. Taken together, these results indicate that GA-T has cytotoxic potency against cancer cells and inhibits their motility *in vitro* by preventing cell-ECM interactions and enhancing cell-cell aggregation. Thus, GA-T may be used therapeutically for the treatment of cancer.

Effect of GA-T on MMP-9, uPA and iNOS protein expression

MMP-9, uPA and iNOS play critical roles in processes associated with tumor invasion, metastasis, and angiogenesis [11, 15, 19, 30, 31]. These enzymes play a major role in facilitating cancer metastasis [2, 19]. In HCT-116 cells, invasive potential has been related to the activity and expression of MMP-9. To determine the effect of GA-T on the expression of MMP-9 protein levels in HCT-116 cells, Western blot analysis was performed. Compared to control treated cells, the inhibition ratio was about 42.3% at 16.3 μM GA-T for 24 h (Fig. 5). Therefore, these data indicate that the treatment of HCT-116 cells with different concentrations of GA-T decreases the amount of MMP-9 protein expressed in a dose-dependent manner.

Angiogenesis is a crucial step in the growth and metastasis of cancer [5]. uPA stimulates cell invasion by cleaving several components of the ECM [11, 25]. uPA is also involved in angiogenesis induced by tu-

mors [19]. Angiogenesis is also initiated through vasodilation mediated by NO [29]. The activation of iNOS catalyzes the production of endogenous NO [15, 23, 29]. Therefore, inhibition of uPA and iNOS expression drastically reduces tumor invasiveness. To determine the effect of GA-T on uPA or iNOS protein expression levels in HCT-116 cells, Western blot analysis was performed using total protein samples extracted from tumor cells. Western blot analysis reveals that GA-T suppresses uPA protein expression at an inhibition ratio of 51.4% at a dose of 32.6 μM GA-T for 24 h (Fig. 6A). Additionally, GA-T suppresses TNFα-induced (1 h) iNOS protein expression at an inhibition ratio of 43.5% at a dose of 16.3 μM GA-T for 24 h (Fig. 6B).

Effect of GA-T on p65 and IκBα protein

As mentioned above, the expression of MMP-9, uPA and iNOS is regulated by the transcription factor NF-κB [11, 15, 23, 27, 31]. To determine whether GA-T inhibits the transactivation of NF-κB, p65 (an important member of the NF-κB family) was detected by western blot. GA-T inhibits the nuclear translocation of p65 at an inhibition ratio of 42.3% and 15.7% at 16.3 μM GA-T for 12 and 24 h, respectively, in HCT-116 cells (Fig. 7). Additionally, GA-T inhibits IκBα degradation. Compared to the controls, the IκBα level was 193.3% upon treatment with 16.3 μM GA-T for 12 h. Therefore, these data indicate that GA-T inhibits NF-κB activity.

Effects of GA-T on inoculated tumor growth and lung metastasis and mRNA expression of MMP-2 and MMP-9 *in vivo*

The LLC model has been extensively studied in both syngeneic and allogeneic mouse models of tumor metastasis. The aim of the present study was to develop a highly metastatic, lung node targeting model of LLC in an allogeneic host that could be imaged. To determine whether GA-T has an anti-tumor effect *in vivo*, a LLC model was established by subcutaneously injecting GA-T into C57BL/6 mice. As shown in Tables 1 and 2, the inhibition rate of tumor growth and lung metastasis of LLC cells in the GA-T-treated group (28 mg/kg) was 63.35% ($p < 0.001$) and 78.33% ($p < 0.001$), respectively. These results demonstrate that GA-T suppresses tumor growth and lung metastasis of LLC cells *in vivo*. The GA-T inhibition rate of tu-

mor growth and lung metastasis was significantly better than GA-Me [32]. However, the molecular mechanism of GA-T inhibition of tumor growth and lung metastasis in mouse was not studied [32].

To investigate whether GA-T inhibits LLC tumor metastasis by reducing MMP-2 and MMP-9 mRNA expression *in vivo*, we performed qRT-PCR analysis of total mRNA from samples extracted from the tumor tissues. Amplification of cDNA using primers specific for human MMP-2, MMP-9 and GAPDH (as a control gene) is shown in Figure 8. The synthesis of MMP-2 and MMP-9 mRNA in tumor tissue was inhibited by GA-T in a dose-dependent manner. Quantitative analysis indicates that 28 mg/kg/day of GA-T could reduce the mRNA level of MMP-2 and MMP-9 to 13.3% ($p < 0.05$) and 6.4% ($p < 0.01$), respectively. These results suggest that GA-T inhibits metastasis by down-regulating the expression of MMP-2 and MMP-9 mRNA.

Discussion

Cancer metastasis is a multi-step process, including migration; homotypic or heterotypic cell-cell adhesions; cell-matrix interactions; invasion into surrounding tissues; release from the primary tumor; intravasation; adhesion to vascular walls; extravasation; and the formation of new foci [36]. Among them, cell adhesion, aggregation, migration, angiogenesis, invasion and metastasis are active areas of research. The work presented here investigated the effect of GA-T on the following processes involved in cancer invasion and metastasis: migration, homotypic and heterotypic cell-cell adhesions, angiogenesis and protease-mediated invasion. To complement our recent work on the anti-cancer effect of GA-T [28], we observed the effects of GA-T on cell aggregation, migration, and adhesion to Matrigel® to further understand the mechanism of the anti-invasion and anti-metastasis effects of GA-T.

A key step in invasion is the attachment of cancer cells to ECM components. Adhesive interactions between tumor cells and ECM components are recognized as playing a critical role in the establishment of invasiveness/metastasis [36]. We assessed the inhibitory effect of GA-T on cell adhesion and aggregation of tumor cells. We first observed that GA-T inhibits Matrigel®-mediated attachment of HCT-116 cells (Fig. 2). When HCT-116 cells were treated with 12.3 μM and 16.3 μM GA-T for 18 h, the adhesion ratios were 64.07.8 ± 3.25% ($p < 0.01$) and 48.02 ± 2.04% ($p < 0.01$), respectively (Fig. 2). Inhibition of tumor adhesion by mixture extracts of *G. lucidum*, as well as the purified compounds GA-A, GA-H and GA-Me, has been reported. However, 0.50 mM GA-A was shown to reduce the adhesion of MDA-MB-231 cells to only 35.9% of the control, while 0.50 mM
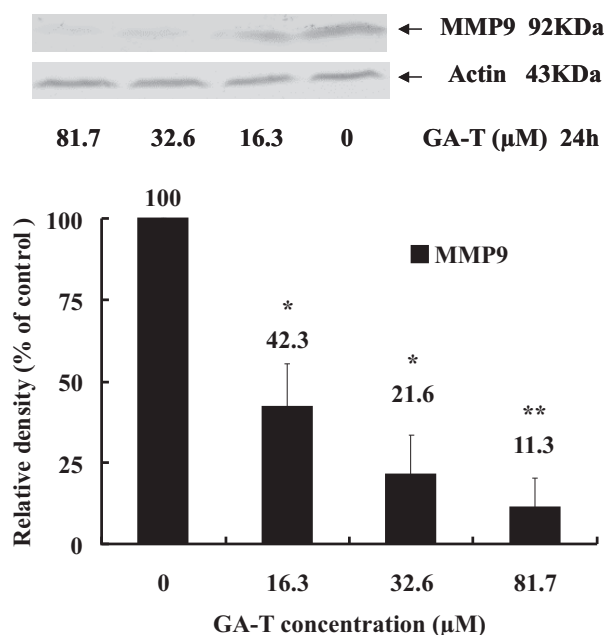

Fig. 5. GA-T reduces the expression of MMP-9 in HCT-116 cells. HCT-116 cells were treated with the indicated concentrations of GA-T for 24 h. Equal amount of total cellular protein were separated on SDS-PAGE and immunoblotted with an anti-MMP-9 antibody and an anti-actin antibody as a loading control. Then the blots were visualized with enhanced chemiluminescence detection and imagined on Kodak TM X-OMAT film. The film was quantitatively measured by scanning densitometry values. Values are expressed as the mean ± SD of three independent experiments and * indicates $p < 0.05$ and ** indicates $p < 0.01$ compared to the untreated (DMSO) control

GA-H decreased the adhesion to only 43.9 % of the control [11]. In the 95-D cells treated with 18.1 μM (10 μg/ml) and 36.2 μM (20 μg/ml) GA-Me for 18 h, the adhesion ratios were $56.8 \pm 3.2\%$ and $20.5 \pm 6.9\%$, respectively [2]. The results presented here provided new information on the effects of *G. lucidum* metabolites on tumor cell adhesion. This decrease in cell adhesion to the ECM might be due to the fact that GA-T inhibits the activity of NF-κB (Fig. 7), which might indirectly suppress focal adhesion kinase activity [8] and thereby reduce cell-matrix adhesion.

Another key step of invasion is homotypic attachment of cancer cells to cells. In normal tissues, cells are tightly associated with one another so that they are generally not allowed to migrate freely. In contrast, malignant cells are more loosely associated and can freely detach from the primary tumor and migrate out. Our results indicate that GA-T facilitates cancer cell adhesion to each other to form aggregates (Fig. 3), which may prevent the initial cell release. Figure 3 shows that GA-T promotes spontaneous cell-cell aggregation in a dose-dependent manner in HCT-116 cells. Until now, the cell homotypic aggregation effect of the triterpene had been unknown. This present work provides new information on the effects of *G. lucidum* metabolites on tumor cell aggregation.

Wound healing assay results indicate that GA-T effectively inhibits migration of HCT-116 cancer cells in a dose-dependent manner (Fig. 4A) and 95-D cancer cells in both a dose- and time-dependent manner (Fig. 4B). These data are consistent with data showing that *G. lucidum* extracts inhibit growth and induce actin polymerization in bladder cancer cells [17]. The anti-invasion effect of GA-T is greater than that of GA-Me. The above results, lead to the conclusion that GA-T effectively inhibits several steps involved in cell invasiveness, including adhesion, aggregation and migration, and thereby inhibits invasiveness of cancer cells.

After the cancer cell has adhered to the ECM, aggregated and migrated, the next key step in the invasive progression is the degradation of a variety of ECM proteins by MMPs. The invasive potential of HCT-116 cells is related to the activity and expression of MMP-2 and MMP-9, which degrade type IV collagen in reconstituted basement membranes. Therefore, we wanted to determine the effect of GA-T on the MMP-9 protein level in HCT-116 cells. Western blot analysis shows that treatment of HCT-116 cells with GA-T results in the down-regulation of MMP-9 pro-
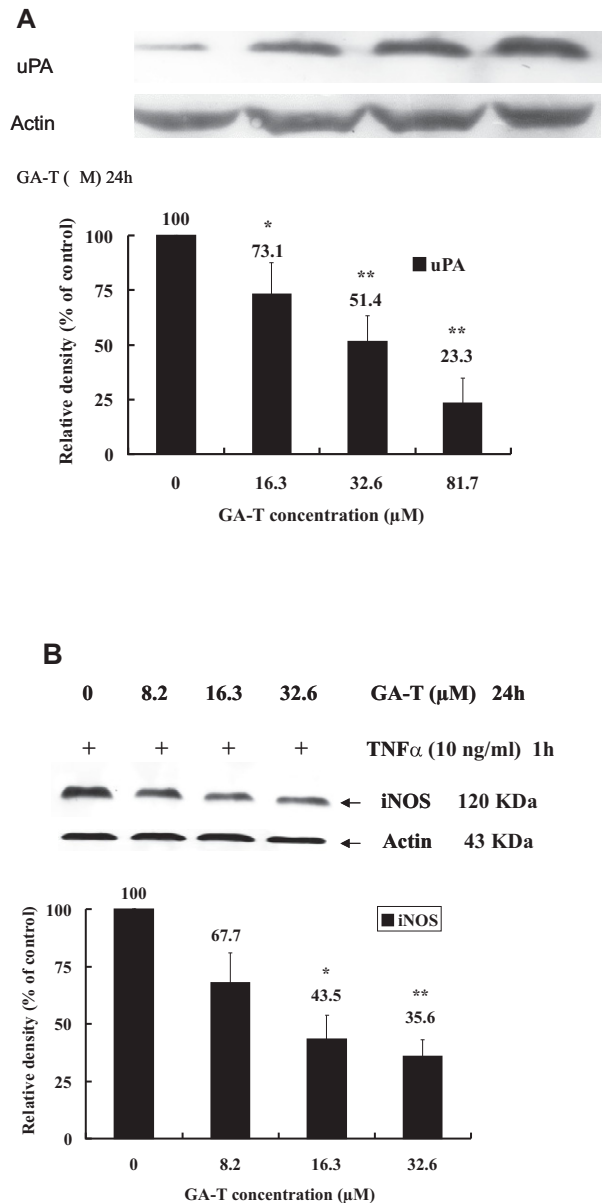

Fig. 6. GA-T reduces the expression of uPA and iNOS proteins in HCT-116 cells. (**A**) uPA expression was determined in HCT-116 cells treated with the indicated concentrations of GA-T for 24 h. (**B**) iNOS expression was determined in HCT-116 cells treated with or without 32.6 μM GA-T for 24 h followed by stimulation with TNFα (10 ng/mL) for 1 h. Equal amount of cellular proteins were separated on SDS-PAGE and blotted with an anti-iNOS or anti-uPA antibody with actin as the loading control. Then the blots were visualized with enhanced chemiluminescence detection and imagined on Kodak TM X-OMAT film. The film was quantitatively measured by scanning densitometry values. Values are expressed as the mean ± SD of three independent experiments where * indicates p < 0.05 and ** indicates p < 0.01 compared to the untreated (DMSO) control

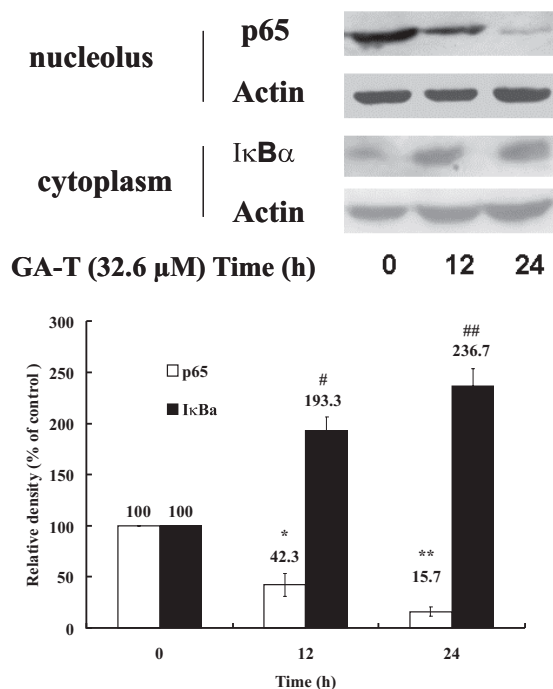tein expression in a dose-dependent manner. These data suggest that GA-T inhibits the invasion of tumor

nucleolus | p65 / Actin

cytoplasm | IκBα / Actin

GA-T (32.6 µM) Time (h)   0   12   24

Tab. 1. GA-T inhibits tumor growth *in vivo*. Tumor weight growth inhibition rate was determined using the following equation: [tumor weight of the control group – tumor weight of the treatment group)/tumor weight of the control group] 100%. The data are expressed as the mean ± SD. One-way ANOVA followed by Dunnett's multiple comparison test were used for statistical analysis, where * indicates $p < 0.05$, ** indicates $p < 0.01$, and *** indicates $p < 0.001$

Groups	N	Dose (mg/kg/day)	Tumor weight (g)	Tumor growth inhibition rate (%)
Negative control	7		1.869 ± 0.517	
Cisplatin (DDP)	7	1	1.045 ± 0.144*	43.9
GA-T (7 mg/kg/day)	7	7	1.355 ± 0.219**	27.5
GA-T (28 mg/kg/day)	7	28	0.685 ± 0.204***	63.3

Tab. 2. GA-T inhibits tumor metastasis *in vivo*. Lung tissues were removed from the animals and the tumor nodes in the surface of lungs were counted under the microscope. Lung metastatic inhibition rate was determined by the following equation: [lung metastatic number of the control group – lung metastatic number of the treatment group)/lung metastatic number of the control group] × 100%. The data are expressed as the mean ± SD. One-way ANOVA followed by Dunnett's multiple comparison test were used for statistical analysis, where ** indicates p 0.01 and *** indicates $p < 0.001$ vs. the negative control

Groups	N	Dose (mg/kg/day)	Number of lung metastases	Lung metastatic inhibition rate (%)
Negative control	7		8.571 ± 1.902	
Cisplatin (DDP)	7	1	1.714 ± 0.488***	80.0
GA-T (7 mg/kg/day)	7	7	5.256 ± 1.799**	38.3
GA-T (28 mg/kg/day)	7	28	1.857 ± 1.069***	78.3

cells by efficiently inhibiting MMP-9 protein expression, similar to the inhibitory effect of GA-Me on MMP-9 [3] (Fig. 5).

Angiogenesis is a crucial step in the growth and metastasis of cancer [5]. Through the proteolytic activity of uPA, uPA activates many angiogenic growth factors, such as bFGF, VEGF, transforming growth factor-β (TGF-β) and fibroblast growth factor (FGF) [11, 19, 25]). uPA also cleaves several components of the ECM, including MMP-2 and MMP-9 [19, 25]. Our results indicate that GA-T suppressed uPA protein expression (Fig. 6A), similar to the inhibitory ef-

fect of GA-A and GA-H on uPA secretion in MDA-MB-231 cells [11]. Angiogenesis is also initiated upon vasodilation mediated by NO [10, 23, 29]. The induction of endogenous NO is catalyzed by iNOS and can cause post-translational modifications of proteins involved in the cell cycle, DNA repair, apoptosis, angiogenesis and invasion/metastasis [23, 29], all of which are associated with the suppression of tumor development and inhibition of metastasis [23]. Therefore, inhibition of uPA and iNOS expression drastically reduces tumor invasiveness. Here, we reveal that

Fig. 8. GA-T decreases the mRNA level of MMP-2 and MMP-9 in LLC tumor tissue in C57B/6 mice. qRT-PCR analysis was carried out after the mice were treated with or without different doses of GA-T. GAPDH was used as the normalized control gene. The procedure is described in the "Materials and Methods". These experiments were repeated independently three times (for each group, n = 3). The data are expressed as the mean ± SD. One-way ANOVA followed by Dunnett's multiple comparison test were used for statistical analysis, where * indicates p < 0.05 and ** indicates p < 0.01 vs. the negative control
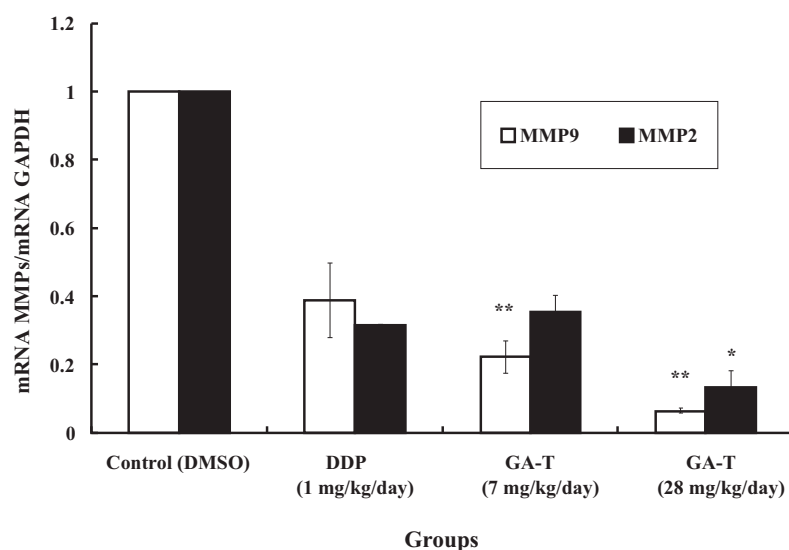
32.6 µM GA-T for 24 h suppresses iNOS protein expression induced by TNFα (Fig. 6B). These data are consistent with *G. lucidum* inhibiting iNOS expression in macrophages [33].

Activation of NF-κB has also been frequently reported to play an important role in pathological processes involved in cancer progression, including cancer cell adhesion, invasion, metastasis, and angiogenesis. Several reports have demonstrated that invasion and migration were induced through the activation of NF-κB and that NF-κB seems to play a central role in regulating the expression of MMP-2, MMP-9, uPA and iNOS [11, 15, 23, 25, 27, 31]. In the present study, we demonstrate that GA-T inhibits MMP-9, uPA and iNOS expression by inhibiting the activity of NF-κB (both the NF-κB nuclear translocation and IκBα degradation) (Fig. 7). These results are consistent with data showing that GA-A and GA-H inhibit the transactivation activity of NF-κB [11, 25] and extracts of *G. lucidum* inhibit the activity of NF-κB (by inhibiting the DNA-binding of NF-κB). However, unique to GA-T is the fact that the different *G. lucidum* extracts do not inhibit IκBα degradation [11]. The different effects of *G. lucidum* extract compounds on IκBα degradation may be the result of which compound(s) in the extract mixture is responsible for the anti-metastasis effect, the fact that different compounds have opposite effects, or due to the use of different cancer cell lines.

Using animals, we demonstrate that GA-T inhibits the growth and metastases of LLC in C57B/6 mice (Tab. 1 and 2). These results were significantly better

than our previous results using GA-Me [32]. Tumor growth inhibition rose from 43.23% for GA-Me (p < 0.05) to 63.35% for GA-T (p < 0.001). Additionally, lung metastatic inhibition rose from 54.89% for GA-Me (p < 0.05) to 78.33% for GA-T (p < 0.001) at a dose of 28 mg/kg. Although GA-Me also inhibited LLC tumor growth and metastases in C57B/6 mice [32], it is unknown whether changes in the expression of the MMP-2 and MMP-9 genes are involved in the inhibition of tumor metastasis *in vivo*. Our results indicate that inhibition of LLC tumor growth and metastases (Tab. 1 and 2) were due to a decrease in the amount of MMP-2 and MMP-9 mRNA expressed in the presence of GA-T (Fig. 8). To our knowledge, this is the first study to show that GA-T effectively inhibits tumor metastasis by inhibiting MMP-2 and MMP-9 mRNA expression *in vivo*.

Our results provide a further in-depth understanding of the molecular mechanisms of the anti-invasion activity of ganoderic acids. Further elucidation of the molecular mechanisms that underlie the anti-invasive and anti-metastasis effects of GA-T are required both *in vivo* and *in vivo*. *Via* over-expression of MMP2/9 (adenovirus) and knockdown of MMP2/9 gene (lentivirus siRNA), we could investigate whether the MMP2/9 is the important target of GA-T of anti-invasion *in vitro* and anti-metastasis *in vivo*.

References:

1. Bielawski K, Bielawska A, Słodownik T, Bołkun-Skórnicka U, Muszyńska A: Proline-linked nitrosoureas as prolidase-convertible prodrugs in human breast cancer cells. Pharmacol Rep, 2008, 60, 171–182.

2. Chen NH, Liu JW, Zhong JJ: Ganoderic acid Me inhibits tumor invasion through down-regulating matrix metalloproteinases 2/9 gene expression. J Pharmacol Sci, 2008, 108, 212–216.

3. Courtois G, Whiteside ST, Sibley CH, Israel A: Characterization of a mutant cell line that does not activate NF-κB in response to multiple stimuli. Mol Cell Biol, 1997, 17, 1441–1449.

4. Du Q, Park KS, Guo Z, He PJ, Nagashima M, Shao LF, Sahai R et al.: Regulation of human nitric oxide synthase 2 expression by Wnt β-catenin signaling. Cancer Res, 2006, 66, 7024–7031.

5. Fukumura D, Jain R: Role of angiogenesis and microcirculation in tumors. Cancer Metastasis Rev. 1998, 17, 77–89.

6. Gao JJ, Hirakawa A, Min BS, Nakamura N, Hattori M: *In vivo* antitumor effects of bitter principles from the antlered form of fruiting bodies of *Ganoderma lucidum*. J Nat Med, 2006, 60, 42–48.

7. Gao JJ, Min BS, Ahn EM, Nakamura N, Lee HK, Hattori M: New triterpene aldehydes, lucialdehydes A-C, from *Ganoderma lucidum* and their cytotoxicity against murine and human tumor cells. Chem Pharm Bull (Tokyo), 2002, 50, 837–840.

8. Golubovskaya V, Kaur A, Cance W: Cloning and characterization of the promoter region of human focal adhesion kinase gene: nuclear factor kappa B and p53 binding sites. Biochim Biophys Acta, 2004, 1678, 111–125.

9. Hsu CL, YU YS, Yen GC: Lucidenic acid B induces apoptosis in human leukemia cells via a mitochondria-mediated pathway. J Agric Food Chem, 2008, 56, 3973–3980.

10. Jenkins DC, Charles IG, Thomsen LL, Moss DW, Holmes LS, Baylis AS, Rhodes P et al.: Roles of nitric oxide in tumor growth. Proc Natl Acad Sci USA, 1995, 92, 4392–4396.

11. Jiang J, Grieb B, Thyagarajan A, Sliva D: Ganoderic acids suppress growth and invasive behavior of breast cancer cells by modulating AP-1 and NF-κB signaling. Int J Mol Med, 2008, 21, 577–584.

12. Kim KC, Kim JS, Son JK, Kim IG: Enhanced induction of mitochondrial damage and apoptosis in human leukemia HL-60 cells by the *Ganoderma lucidum* and *Duchesnea chrysantha* extracts. Cancer Lett, 2007, 246, 210–217.

13. Kimura Y, Taniguchi M, Baba K: Antitumor and antimetastatic effects on liver of triterpenoid fractions of *Ganoderma lucidum*: mechanism of action and isolation of an active substance. Anticancer Res, 2002, 22, 3309–3318.

14. Li CH, Chen PY, Chang UM, Kan LS, Fang WH, Tsai KS, Lin SB: Ganoderic acid X, a lanostanoid triterpene, inhibits topoisomerases and induces apoptosis of cancer cells. Life Sci, 2005, 77, 252–265.

15. Liu J, Zhan MC, Hannay JAF, Das P, Bolshakov SV, Kotilingam D, Yu DH et al.: Wild-type p53 inhibits nuclear factor-κB-induced matrix metalloproteinase-9 promoter activation: implications for soft tissue sarcoma growth and metastasis. Mol Cancer Res, 2006, 4, 803–810.

16. Livak K, Schmittgen TD: Analysis of relative gene expression data using real-time quantitative PCR and the $2^{-\Delta\Delta Ct}$ method. Methods, 2001, 25, 402–408.

17. Lu QY, Jin YS, Zhang QF, Zhang ZF, Heber D, Go VLW, Li FP, Rao JY: *Ganoderma lucidum* extracts inhibit growth and induce actin polymerization in bladder cancer cells *in vitro*. Cancer Lett, 2004, 216, 9–20.

18. Małek R, Borowicz KK, Jargiełło M, Czuczwar SJ: Role of nuclear factor κB in the central nervous system. Pharmacol Rep, 2007, 59, 25–33.

19. Mazar AP, Henkin J, Goldfarb RH: The urokinase plasminogen activator system in cancer: implications for tumor angiogenesis and metastasis. Angiogenesis, 1999, 3, 15–32.

20. Min BS, Gao JJ, Nakamura N, Hattori M: Triterpenes from the spores of *Ganoderma lucidum* and their cytotoxicity against meth-A and LLC tumor cells. Chem Pharm Bull (Tokyo), 2000, 48, 1026–1033.

21. Philip S, Kundu GC: Osteopontin induces nuclear factor κB-mediated promatrix metalloproteinase-2 activation through IκBα/IKK signaling pathways, and curcumin (diferulolylmethane) down-regulates these pathways J Biol Chem, 2003, 278, 14487–14497.

22. Pilarski R, Poczekaj-Kostrzewska M, Ciesiołka D, Szyfter K, Gulewicz K: Antiproliferative activity of various *Uncaria tomentosa* preparations on HL-60 promyelocytic leukemia cells. Pharmacol Rep, 2007, 59, 565–572.

23. Rao CV, Indranie C, Simi B, Manning PT, Connor JR, Reddy BS: Chemopreventive properties of a selective inducible nitric oxide synthase inhibitor in colon carcinogenesis, administered alone or in combination with celecoxib, a selective cyclooxygenase-2 inhibitor. Cancer Res, 2002, 62, 165–170.

24. Russell R, Paterson M: Ganoderma – A therapeutic fungal biofactory. Phytochemistry, 2006, 67, 1985–2001.

25. Sliva D, Labarrere C, Slivova V, Sedlak M, Lloyd FP, Ho NWY: *Ganoderma lucidum* suppresses motility of highly invasive breast and prostate cancer cells. Biochem Biophys Res Commun, 2002, 298, 603–612.

26. Stanley G, Harvey K, Slivova V, Jiang JH, Sliva D: *Ganoderma lucidum* suppresses angiogenesis through the inhibition of secretion of VEGF and TGF-β1 from prostate cancer cells. Biochem Biophys Res Commun, 2005, 330, 46–52.

27. Sun Z, Andersson R: NF-κB activation and inhibition: a review. SHOCK, 2002, 18, 99–106.

28. Tang W, Liu JW, Zhao WM, Wei D.Z, Zhong JJ: Ganoderic acid T from *Ganoderma lucidum* mycelia induces mitochondria mediated apoptosis in lung cancer cells. Life Sci, 2006, 80, 205–211.

29. Thejass P, Kuttan G: Allyl isothiocyanate (AITC) and phenyl isothiocyanate (PITC) inhibit tumour-specific

angiogenesis by downregulating nitric oxide (NO) and tumour necrosis factor-α (TNF-α) production. Nitric Oxide, 2007, 16, 247–257.

30. Thyagarajan A, Jiang J, Hopf A, Adamec J, Sliva D: Inhibition of oxidative stress-induced invasiveness of cancer cells by *Ganoderma lucidum* is mediated through the suppression of interleukin-8 secretion. Int J Mol Med, 2006, 18, 657–664.

31. Van Waes C: Nuclear factor-κB in development, prevention, and therapy of cancer. Clin Cancer Res, 2007, 13, 1076–1082.

32. Wang G, Zhao J, Liu JW, Huang YP, Zhong JJ, Tang W: Enhancement of IL-2 and IFN-γ expression and NK cells activity involved in the anti-tumor effect of ganoderic acid Me *in vivo*. Int Immunopharmacol, 2007, 7, 864–870.

33. Woo CWH, Man RYK, Siow YL, Choy PC, Wan EWY, Lau CS, Karmin O: *Ganoderma lucidum* inhibits inducible nitric oxide synthase expression in macrophages. Mol Cell Biochem, 2005, 275, 165–171.

34. Wu QP, Xie YZ, Li SZ, La Pierre DP, Deng Z, Chen Q, Li C et al. : Tumor cell adhesion and integrin expression affected by *Ganoderma lucidum*. Enzyme Microb Tech, 2006, 40, 32–41.

35. Yue QX, Cao ZW, Guan SH, Liu XH, Tao L, Wu WY, Li YX et al.: Proteomics characterization of the cytotoxicity mechanism of ganoderic acid D and computer-automated estimation of the possible drug target network. Mol Cell Proteomics, 2008, 7, 949–961.

36. Zhang J, Shen YL, Liu JW, Wei DZ: Antimetastatic effect of prodigiosin through inhibition of tumor invasion. Biochem Pharmacol, 2005, 69, 407–414.